

Monte Carlo wave-function method in quantum optics

Klaus Mølmer

Institute of Physics and Astronomy, University of Aarhus, DK-8000 Aarhus C, Denmark

Yvan Castin and Jean Dalibard

Laboratoire de Spectroscopie Hertzienne de l'Ecole Normale Supérieure, 24 rue Lhomond, F-75231 Paris Cedex 05, France

Received April 7, 1992; revised manuscript received July 8, 1992

We present a wave-function approach to the study of the evolution of a small system when it is coupled to a large reservoir. Fluctuations and dissipation originate in this approach from quantum jumps that occur randomly during the time evolution of the system. This approach can be applied to a wide class of relaxation operators in the Markovian regime, and it is equivalent to the standard master-equation approach. For systems with a number of states N much larger than unity this Monte Carlo wave-function approach can be less expensive in terms of calculation time than the master-equation treatment. Indeed, a wave function involves only N components, whereas a density matrix is described by N^2 terms. We evaluate the gain in computing time that may be expected from such a formalism, and we discuss its applicability to several examples, with particular emphasis on a quantum description of laser cooling.

1. INTRODUCTION

The problem of dissipation plays a central role in quantum optics. The simplest example is the phenomenon of spontaneous emission, in which the coupling between an atom and the ensemble of modes of the quantized electromagnetic field gives a finite lifetime to all excited atomic levels. Usually the dissipative coupling between a small system and a large reservoir can be treated by a master-equation approach¹⁻⁴; one writes a linear equation for the time evolution of the reduced system density matrix, $\rho_S = \text{Tr}_{\text{res}}(\rho)$, trace over the reservoir variables of the total density matrix. If we denote the Hamiltonian for the isolated system H_S , this equation can be written as

$$\dot{\rho}_S = (i/\hbar)[\rho_S, H_S] + \mathcal{L}_{\text{relax}}(\rho_S). \quad (1)$$

In Eq. (1), $\mathcal{L}_{\text{relax}}$ is the relaxation superoperator, acting on the density operator ρ_S . It is assumed here to be local in time, which means that $\dot{\rho}_S(t)$ depends only on ρ_S at the same time (Markov approximation). All the system dynamics can be deduced from Eq. (1). One can calculate one-time average values of a system operator A : $a(t) = \langle A \rangle(t) = \text{Tr}[\rho_S(t)A]$ and also, by using the quantum regression theorem,⁵ multitime correlation functions, such as $\langle A(t + \tau)B(t) \rangle$.

Recently a novel treatment of dissipation of energy from a quantum system (two-level atom) coupled to a zero-temperature reservoir was presented.⁶ This treatment is based on the evolution of a Monte Carlo wave function (MCWF) of the small system, which consists of two elements: evolution with a non-Hermitian Hamiltonian and randomly decided quantum jumps, followed by wave-function renormalization. This approach, which is equivalent to the master-equation treatment, is interesting for two reasons. First, if the relevant Hilbert space of the quantum system has a dimension N that is large compared with 1, the number of variables involved in a wave-

function treatment ($\sim N$) is much smaller than the one required for calculations with density matrices ($\sim N^2$). Second, new physical insight may be gained, in particular in the studies of the behavior of a single-quantum system.

The purpose of the present paper is to give a general presentation of this method for a wide class of system-reservoir couplings (Section 2). In particular, the method presented here is not restricted to a zero-temperature reservoir. The physical content of the method and its relation to previous wave-function treatments in dissipative quantum optics are discussed in Section 3. We then indicate how the MCWF formalism can be used for calculating two-time correlation functions, and we give two illustrations of this (Section 4). Section 5 is devoted to the presentation of a series of examples to which the MCWF treatment can be applied. In Section 6 we discuss the existence of several MCWF descriptions for a given relaxation operator $\mathcal{L}_{\text{relax}}$, and we illustrate this with an example of population trapping. Finally, in Section 7 we give a few indications concerning the convergence of the MCWF method and the gain in computing time that one might expect.

Soon after the completion of the study by Dalibard *et al.*⁶ it was brought to our attention that other approaches have recently been developed involving a stochastic evolution of wave functions. In the context of nonclassical field generation, Carmichael⁷ proposed an approach named quantum trajectories, inspired by the theory of photoelectron-counting sequences⁸ and quite similar to the spirit of Dalibard *et al.*⁶ On the basis of the continuous quantum theory of measurement,⁹ Dum *et al.*¹⁰ developed a Monte Carlo simulation of the atomic master equation for spontaneous emission. In the framework of quantum jump theory, Hegerfeldt and Wilser¹¹ considered a quantum-mechanical model for describing a single radiating atom, which could also be the starting point for an effective Monte Carlo evolution with atomic wave func-

tions.¹¹ Finally, the relation of Ref. 6 to a general stochastic formulation of quantum mechanics has been pointed out to us by Gisin.¹² Throughout this paper we will connect our results with the ones obtained in these parallel approaches.

2. GENERAL PRESENTATION OF THE METHOD

In this section we present a general description of the MCWF method. We start by presenting the class of relaxation operators that can be studied by this method. We then present the procedure itself, and finally we show its equivalence with the master-equation treatment.

A. Relaxation Operator

The class of relaxation operators that we consider in this paper is the following:

$$\mathcal{L}_{\text{relax}}(\rho_S) = -\frac{1}{2} \sum_m (C_m^\dagger C_m \rho_S + \rho_S C_m^\dagger C_m) + \sum_m C_m \rho_S C_m^\dagger. \quad (2)$$

This type of relaxation operator is quite general and is found in most of the quantum optics problems involving dissipation. In Eq. (2) the C_m operators act in the space of the small system. Depending on the nature of the problem there can be one, a few, or an infinity of these operators.

A series of examples with the dissipation operator in the form of Eq. (2) will be given in Section 5. Here we indicate the expression of $\mathcal{L}_{\text{relax}}(\rho_S)$ for the case of spontaneous emission by a two-level system or by a harmonic oscillator, where there is just a single operator $C_1 = \sqrt{\Gamma} \sigma^-$ in the relaxation operator [Eq. (2)]:

$$\mathcal{L}_{\text{relax}}(\rho_S) = -(\Gamma/2)(\sigma^+ \sigma^- \rho_S + \rho_S \sigma^+ \sigma^-) + \Gamma \sigma^- \rho_S \sigma^+. \quad (3)$$

For the two-level system formed with a stable ground state $|g\rangle$ and an excited state $|e\rangle$ with a lifetime Γ^{-1} , we have

$$\sigma^+ = S^+ = |e\rangle\langle g|, \quad \sigma^- = S^- = |g\rangle\langle e|. \quad (4)$$

For a harmonic oscillator, σ^- and σ^+ are related to lowering and raising operators:

$$\sigma^- = b, \quad \sigma^+ = b^\dagger. \quad (5)$$

B. Monte Carlo Wave-Function Procedure

We now present the procedure for evolving wave functions of the small system. Consider at time t that the system is in a state with the normalized wave function $|\phi(t)\rangle$. In order to get the wave function at time $t + \delta t$, we proceed in two steps:

1. We calculate the wave function $|\phi^{(1)}(t + \delta t)\rangle$ obtained by evolving $|\phi(t)\rangle$ with the non-Hermitian Hamiltonian:

$$H = H_S - \frac{i\hbar}{2} \sum_m C_m^\dagger C_m. \quad (6)$$

This gives the following for sufficiently small δt :

$$|\phi^{(1)}(t + \delta t)\rangle = \left(1 - \frac{iH\delta t}{\hbar}\right) |\phi(t)\rangle. \quad (7)$$

Since H is not Hermitian, this new wave function clearly is not normalized. The square of its norm is

$$\begin{aligned} \langle \phi^{(1)}(t + \delta t) | \phi^{(1)}(t + \delta t) \rangle &= \langle \phi(t) | \left(1 + \frac{iH^\dagger \delta t}{\hbar}\right) \left(1 - \frac{iH\delta t}{\hbar}\right) | \phi(t) \rangle \\ &= 1 - \delta p, \end{aligned} \quad (8)$$

where δp reads as

$$\delta p = \delta t \frac{i}{\hbar} \langle \phi(t) | H - H^\dagger | \phi(t) \rangle = \sum_m \delta p_m, \quad (9)$$

$$\delta p_m = \delta t \langle \phi(t) | C_m^\dagger C_m | \phi(t) \rangle \geq 0. \quad (10)$$

The magnitude of the step δt is adjusted so that this calculation at first order is valid; in particular, it requires $\delta p \ll 1$.

2. The second step of the evolution of $|\phi\rangle$ between t and $t + \delta t$ consists in a possible quantum jump. We leave this term intentionally vague here; for particular examples we see below that this quantum jump can correspond to the projection of the wave function associated with a *gedanken* measurement process. In order to decide whether this jump happens, we choose a quasi-random number ϵ , uniformly distributed between 0 and 1, and we compare it with δp . If δp is smaller than ϵ , which occurs in most cases since $\delta p \ll 1$, no quantum jump occurs, and we take the following for the new normalized wave function at $t + \delta t$:

$$|\phi(t + \delta t)\rangle = |\phi^{(1)}(t + \delta t)\rangle / (1 - \delta p)^{1/2}, \quad \delta p < \epsilon. \quad (11)$$

If $\epsilon < \delta p$, a quantum jump occurs, and we choose the new normalized wave function among the different states $C_m |\phi(t)\rangle$, according to the probability law $\Pi_m = \delta p_m / \delta p$ [note that $\sum_m \Pi_m = 1$ because of Eq. (9)]:

$$|\phi(t + \delta t)\rangle = C_m |\phi(t)\rangle / (\delta p_m / \delta t)^{1/2} \quad \text{with a probability } \Pi_m = \delta p_m / \delta p, \quad \delta p > \epsilon. \quad (12)$$

For the particular case of a two-level atom coupled to the vacuum electromagnetic field, these two steps coincide with the ones given in Refs. 6 and 7.

C. Equivalence with the Master Equation

With this set of rules we can propagate a wave function $|\phi(t)\rangle$ in time, and we now show that this procedure is equivalent to the master equation (1). More precisely, we consider the quantity $\bar{\sigma}(t)$ obtained by averaging $\sigma(t) = |\phi(t)\rangle\langle\phi(t)|$ over the various possible outcomes at time t of the MCWF evolutions all starting in $|\phi(0)\rangle$, and we prove that $\bar{\sigma}(t)$ coincides with $\rho_S(t)$ at all times t , provided that they coincide at $t = 0$.

Consider a MCWF $|\phi(t)\rangle$ at time t . At time $t + \delta t$ the average value of $\sigma(t + \delta t)$ over the evolution caused by different values of the random number ϵ is

$$\begin{aligned} \overline{\sigma(t + \delta t)} &= (1 - \delta p) \frac{|\phi^{(1)}(t + \delta t)\rangle \langle \phi^{(1)}(t + \delta t)|}{(1 - \delta p)^{1/2} (1 - \delta p)^{1/2}} \\ &+ \delta p \sum_m \Pi_m \frac{C_m |\phi(t)\rangle \langle \phi(t)| C_m^\dagger}{(\delta p_m / \delta t)^{1/2} (\delta p_m / \delta t)^{1/2}}, \end{aligned} \quad (13)$$

which gives, when we use Eq. (7),

$$\overline{\sigma(t + \delta t)} = \sigma(t) + (i\delta t/\hbar)[\sigma(t), H_S] + \delta t \mathcal{L}_{\text{relax}}[\sigma(t)]. \quad (14)$$

We now average this equation over the possible values of $\sigma(t)$, and we obtain

$$\frac{d\bar{\sigma}}{dt} = \frac{i}{\hbar}[\bar{\sigma}, H_S] + \mathcal{L}_{\text{relax}}(\bar{\sigma}). \quad (15)$$

This equation is identical to the master equation (1). If we assume that $\rho_S(0) = |\phi(0)\rangle\langle\phi(0)|$, $\bar{\sigma}(t)$ and $\rho_S(t)$ coincide at any time, which demonstrates the equivalence between the two points of view. In the case where $\rho_S(0)$ does not correspond to a pure state, one first has to decompose it as a statistical mixture of pure states, $\rho(0) = \sum p_i |\chi_i\rangle\langle\chi_i|$, and then randomly choose the initial MCWF's among the $|\chi_i\rangle$ with the probability law p_i .

As is mentioned in Section 1, the master-equation approach and the reduced density matrix give access to one-time average values $a(t) = \langle A \rangle(t) = \text{Tr}[\rho_S(t)A]$, which can now also be obtained with the MCWF method. For several outcomes $|\phi^{(i)}(t)\rangle$ of the MCWF evolution, one calculates the quantum average $\langle \phi^{(i)}(t) | A | \phi^{(i)}(t) \rangle$, and one takes the mean value of this quantity over the various outcomes $|\phi^{(i)}(t)\rangle$:

$$\langle A \rangle_{(n)}(t) = \frac{1}{n} \sum_{i=1}^n \langle \phi^{(i)}(t) | A | \phi^{(i)}(t) \rangle. \quad (16)$$

For n values that are sufficiently large, Eq. (15) implies that $\langle A \rangle_{(n)}(t) \approx \langle A \rangle(t)$. We will see in Sections 5 and 7 that this MCWF procedure based on the use of Eq. (16) for determining average values of operators may be more efficient than the master-equation approach.

It appears clearly in this proof that the equivalence of the master-equation and MCWF approaches does not depend on the particular value of the time step δt . From a practical point of view, the largest possible δt is preferable, and one might benefit from using a generalization of Eq. (7) to a higher order in δt , for example, a fourth-order Runge-Kutta-type calculation. The only requirement on δt is that the various $\eta_i \delta t$, where the $\hbar \eta_i$ are the eigenvalues of H , should be small compared with 1. Of course, we assume here that those eigenvalues have been simplified as much as possible in order to eliminate the bare energies of the eigenstates of H_S . For instance, for a two-level atom with a transition frequency ω_A coupled to a laser field with frequency ω_L , one makes the rotating-wave approximation in the rotating frame so that the $|\eta_i|$ values are of the order of the natural width Γ , the Rabi frequency Ω , or the detuning $\delta = \omega_L - \omega_A$; they are consequently much smaller than ω_A .

One might wonder whether there is a minimal size for the time step δt . In the derivation presented above, it can be chosen to be arbitrarily small. However, one should remember that the derivation of Eq. (1) involves a coarse-grain average of the real density operator evolution. The time step of this coarse-grain average has to be much larger than the correlation time τ_c of the reservoir, which is typically an optical period for the problem of spontaneous emission. Therefore one should be cautious when considering any result derived from this MCWF approach involving details with a time scale of the order of or

shorter than τ_c , and only δt larger than τ_c should be applied. This appears clearly if one starts directly from the interaction Hamiltonian between the system and the reservoir in order to generate the stochastic evolution for the system wave function.⁶ The condition $\delta t \gg \tau_c$ is then necessary to prevent quantum Zeno-type effects.¹³ This restriction is discussed in detail in Ref. 11 in connection with quantum measurement theory.

3. PHYSICAL INTERPRETATION OF THIS PROCEDURE

We now discuss the physical content of this procedure. To this purpose, we consider at time $t = 0$ a harmonic oscillator (the same formalism applies to the case of a two-level system by replacement of $|0\rangle$ and $|1\rangle$ by $|g\rangle$ and $|e\rangle$) in a superposition of the two lowest-lying states:

$$|\phi(0)\rangle = \alpha_0|0\rangle + \beta_0|1\rangle. \quad (17)$$

We suppose that the oscillator relaxes toward its ground state $|0\rangle$ with the relaxation operator defined by Eqs. (3) and (5). Therefore we know that at time $t = +\infty$ the oscillator will be in state $|0\rangle$; it may have reached this state without emitting any photon (probability $|\alpha_0|^2$) or with the emission of one single photon (probability $|\beta_0|^2$).

In the MCWF formalism, following the first step of Subsection 2.B and using $H_S = \hbar\omega_0 b^\dagger b$, we have at time δt

$$|\phi^{(i)}(\delta t)\rangle = \alpha_0|0\rangle + \beta_0 \exp(-i\omega_0\delta t) \exp(-\Gamma\delta t/2)|1\rangle. \quad (18)$$

The probability δp defined in Eq. (9) for making a quantum jump is

$$\delta p = \Gamma|\beta_0|^2\delta t, \quad (19)$$

and it corresponds to the probability for emitting a photon between 0 and δt . The choice of the random number ϵ therefore simulates the result of the measurement of the number of photons emitted between 0 and δt . The case $\delta p > \epsilon$ corresponds to the detection of a photon, and the quantum jump described in Eq. (12) is simply the projection of the wave function onto the ground state $|0\rangle$, associated with this detection. If such a quantum jump occurs, the wave function $|\phi(\delta t)\rangle$ is simply $|0\rangle$, and it does not evolve anymore.

We now investigate the other part of the wave-function evolution, i.e., the case $\delta p < \epsilon$, corresponding to the no-detection result. First, we treat the example of the harmonic oscillator. Then we consider the general result and connect it with previous wave-function treatments in quantum optics, mainly on the basis of the delay function (or waiting time function).

If no quantum jump occurs, the normalized wave function $|\phi(\delta t)\rangle$ is proportional to $|\phi^{(i)}(\delta t)\rangle$. Using the fact that δt is small, we get

$$\begin{aligned} |\phi(\delta t)\rangle = & \alpha_0 \left(1 + \frac{\Gamma\delta t}{2} |\beta_0|^2 \right) |0\rangle \\ & + \beta_0 \left(1 - \frac{\Gamma\delta t}{2} |\alpha_0|^2 \right) \exp(-i\omega_0\delta t) |1\rangle, \quad \delta p < \epsilon. \end{aligned} \quad (20)$$

We note that in addition to the free evolution at frequency

ω_0 , there has been a slight rotation of the wave function: the probability amplitude of being in the ground state has increased, and the probability of being in the first excited state has decreased. From the photon measurement point of view, the non-Hermitian part of the evolution described in Subsection 2.B corresponds to the modification of the state of the system associated with a no-detection result of the number of emitted photons. The information gained in a zero-result experiment and its consequences for the evolution of the system has been emphasized by Dicke,¹⁴ and, in the context of quantum jumps, by Pegg and Knight,¹⁵ by Cook,¹⁶ and by Porrati and Putterman.¹⁷ For the present problem this rotation is essential. If it did not occur, i.e., if we were to take

$$|\phi(\delta t)\rangle = \alpha_0|0\rangle + \beta_0 \exp(-i\omega_0\delta t)|1\rangle, \quad \delta p < \epsilon, \quad (21)$$

the probability of having a quantum jump (i.e., detecting a photon) between δt and $2\delta t$ would be strictly equal to the probability between 0 and δt [Eq. (19)], and this would repeat over and over until a quantum jump would finally occur. One would then always find that a photon is emitted between $t = 0$ and $t = \infty$, provided that $|\beta_0|^2 \neq 0$, and this conclusion would clearly be wrong. Owing to the slight rotation in Eq. (20), however, the probability for making a quantum jump between δt and $2\delta t$ is smaller than δp , and it will be reduced over and over, as no quantum jump occurs in successive time steps. Assuming that no quantum jump occurred between 0 and t , we can write $|\phi(t)\rangle$ as

$$|\phi(t)\rangle = \alpha(t)|0\rangle + \beta(t) \exp(-i\omega_0 t)|1\rangle, \quad (22)$$

where $\alpha(t)$ and $\beta(t)$ are solutions of the nonlinear set of equations deduced from Eq. (20):

$$\begin{aligned} \dot{\alpha} &= \Gamma\alpha|\beta|^2/2, \\ \dot{\beta} &= -\Gamma\beta|\alpha|^2/2. \end{aligned} \quad (23)$$

The solution of this set of equations is

$$\begin{aligned} \alpha(t) &= \alpha_0[|\alpha_0|^2 + |\beta_0|^2 \exp(-\Gamma t)]^{-1/2}, \\ \beta(t) &= \beta_0 \exp(-\Gamma t/2)[|\alpha_0|^2 + |\beta_0|^2 \exp(-\Gamma t)]^{-1/2}. \end{aligned} \quad (24)$$

The probability $P(t)$ for having no quantum jumps between 0 and t is found to be

$$P(t) = |\alpha_0|^2 + |\beta_0|^2 \exp(-\Gamma t). \quad (25)$$

This confirms the statement made at the beginning of this section: there is a probability $|\alpha_0|^2$ that no jump will occur between $t = 0$ and $t = \infty$, and there is a probability $|\beta_0|^2 = 1 - |\alpha_0|^2$ for a jump to occur. In this particular case we have therefore been able to determine completely the stochastic evolution of $|\phi(t)\rangle$ (see also Ref. 7):

With a probability $P(t)$,

$$|\phi(t)\rangle = \alpha(t)|0\rangle + \beta(t)\exp(-\omega_0 t)|1\rangle; \quad (26a)$$

With a probability $1 - P(t)$,

$$|\phi(t)\rangle = |0\rangle, \quad (26b)$$

where $\alpha(t)$ and $\beta(t)$ are given in Eqs. (24). We note that if the initial state of the oscillator is taken as an eigenstate

of b , a coherent state, the wave function is not changed in quantum jumps, and all changes take place during the nonunitary evolution, which takes the wave function through a progression of coherent states (see also Ref. 12).

We now extend this treatment of the zero quantum jump periods to the general case. Suppose that we know that no quantum jump has occurred between 0 and t . During this period we find that the wave function obeys a nonlinear differential equation deduced from Eqs. (7) and (11):

$$i\hbar \frac{d|\phi\rangle}{dt} = \left(H + \langle\phi|\frac{H^\dagger - H}{2}|\phi\rangle \right) |\phi\rangle, \quad (27)$$

which generalizes Eqs. (23). The solution of this equation is, for a time-independent Hamiltonian,

$$\begin{aligned} |\phi(t)\rangle &= \langle\phi(0)|\exp(iH^\dagger t/\hbar)\exp(-iHt/\hbar)|\phi(0)\rangle^{-1/2} \\ &\times \exp(-iHt/\hbar)|\phi(0)\rangle, \end{aligned} \quad (28)$$

which generalizes Eqs. (24). This corresponds to an evolution with the non-Hermitian Hamiltonian between 0 and t :

$$i\hbar \frac{d|\phi\rangle}{dt} = H|\phi\rangle \quad (29)$$

and a normalization of the result at the end of the evolution.

This result allows us to connect our approach to the standard treatments of resonance fluorescence. In those treatments, following the work of Mollow,¹⁸ the atomic dynamics is interpreted as phases of evolution with a non-Hermitian Hamiltonian H , separated by spontaneous-emission processes. This non-Hermitian Hamiltonian coincides with the one derived in this paper for the particular case of spontaneous emission. If one defines a reduced atomic density operator $\sigma^{(n)}(t)$ in the subspace containing $n = 0, 1, 2, \dots$, fluorescence photons, one gets an infinite hierarchy of equations¹⁸:

$$\frac{d\sigma^{(n)}}{dt} = \frac{i}{\hbar}[\sigma^{(n)}, H] + \text{feeding term}(\sigma^{(n-1)}), \quad (30)$$

which corresponds to the atom cascading along the ladder labeled by the number of fluorescence photons $n = 0, 1, 2, \dots$.

This picture has been used successfully to interpret many quantum-optics phenomena, such as resonance fluorescence spectra, photon statistics, and quantum jumps. In this formalism an important quantity is the probability distribution of the time interval between the emissions of two successive photons, i.e., the so-called delay function or waiting time function.¹⁹⁻²¹ When this function is known analytically, it can generate an efficient Monte Carlo analysis of the process: just after the emission of the n th fluorescence photon at time t_n , the atom is in its ground state and the choice of a single random number is sufficient to determine the time t_{n+1} of emission of the $(n+1)$ th photon. This type of Monte Carlo analysis was used in Ref. 22 to simulate an atomic-beam cooling experiment and in Ref. 20 to prove numerically the existence of dark periods in the fluorescence of a three-level atom (quantum jumps). Recently laser cooling of atoms

by velocity-selective coherent population trapping²³ and lasing without inversion²⁴ have been analyzed by this type of Monte Carlo method.

Unfortunately the delay function cannot be calculated analytically for complex systems that involve a large number of levels. Nevertheless, it is possible to generate a Monte Carlo solution of Eq. (30) in which a single random number determines the time of emission of each fluorescence photon.¹⁰ The non-Hermitian evolution given in Eq. (29) has to be integrated step by step numerically, so that the amount of calculation involved is similar to that required by the method presented in this paper. The physical interpretations of the two approaches are also similar; we note in particular that for both approaches physical quantities such as $\langle \phi(t)|A|\phi(t) \rangle$ have to be evaluated with normalized wave functions. This normalization is systematically done at every step for the approach presented in this paper and has to be added in the approach based on the numerical simulation of Eq. (30).

Finally, we note that, as was shown in Gisin,¹² it is also possible to simulate a relaxation equation of the type of Eqs. (1) and (2) by a continuous stochastic equation (see also Ref. 25). In this approach, no quantum jump occurs, but at each step δt a small random element is added to the wave function. This approach has been used mainly in a discussion of the foundations of quantum mechanics, but it can also be the starting point for an explicit solution to quantum optics problems.²⁶ For the particular case of homodyne detection of fluorescence light, Carmichael⁷ has transformed the evolution involving quantum jumps (Subsection 2.B) into a continuous stochastic evolution similar to the one obtained by Gisin.

4. TWO-TIME CORRELATION FUNCTION

Often in quantum optics problems one needs to calculate two-time correlation functions of atomic operators A and B , such as

$$C(t, \tau) = \langle A(t + \tau)B(t) \rangle. \quad (31)$$

For instance, the fluorescence spectrum of a laser-driven atomic system is obtained by the Fourier transform of the two-time correlation function of the dipole. Another example in the semiclassical theory of radiative forces is the momentum diffusion coefficient, which describes the heating of the atom caused by the fluctuations that are due to the randomness of spontaneous-emission processes and which is given by the integral of the two-time correlation function of the force operator. The goal of this section is to indicate how one can handle such a calculation in the MCWF method and to give some examples of this procedure.²⁷

A. Master-Equation Approach to Correlation Functions

In the master-equation approach, correlation functions such as the one in Eq. (31) are calculated by using the quantum regression theorem⁵: one expands A on the basis of $X_{ij} = |i\rangle\langle j|$, where $|i\rangle$ and $|j\rangle$ are members of a basis set of the system Hilbert space, and one calculates the value of the corresponding correlation functions:

$$C_{ij}(t, \tau) = \langle X_{ij}(t + \tau)B(t) \rangle. \quad (32)$$

For $\tau = 0$ the $C_{ij}(t, 0)$ are one-time averages and are calculated directly from the master-equation result for the density matrix. The τ evolution of the $C_{ij}(t, \tau)$ is shown to be given by

$$\frac{\partial C_{ij}}{\partial \tau}(t, \tau) = \sum_{kl} \mathcal{L}_{ijkl} C_{kl}(t, \tau), \quad (33)$$

where the coefficients \mathcal{L}_{ijkl} , which include the evolution that is due to the system Hamiltonian as well as the contribution of \mathcal{L}_{relax} , are the same as the ones giving the evolution of the one-time averages (quantum regression theorem):

$$\frac{d\langle X_{ij}(t) \rangle}{dt} = \sum_{kl} \mathcal{L}_{ijkl} \langle X_{kl}(t) \rangle. \quad (34)$$

These one-time averages $\langle X_{ij}(t) \rangle$ are identical to the density-matrix elements $\rho_{ji}(t)$; the coefficients \mathcal{L}_{ijkl} are accordingly known from the master equation (1), and one readily solves Eq. (33).

B. Monte-Carlo Approach

We now present the procedure that one can use in the MCWF formalism. We first let $|\phi\rangle$ evolve from 0 to t , as explained in Section 2. For a given outcome $|\phi(t)\rangle$ of this evolution we form the four new states:

$$|\chi_{\pm}(0)\rangle = \frac{1}{\sqrt{\mu_{\pm}}} (1 \pm B)|\phi(t)\rangle, \quad (35)$$

$$|\chi'_{\pm}(0)\rangle = \frac{1}{\sqrt{\mu'_{\pm}}} (1 \pm iB)|\phi(t)\rangle, \quad (36)$$

where μ_{\pm} , μ'_{\pm} are normalization coefficients. Now evolving $|\chi_{\pm}(\tau)\rangle$ and $|\chi'_{\pm}(\tau)\rangle$ according to the MCWF procedure, we calculate

$$c_{\pm}(\tau) = \langle \chi_{\pm}(\tau) | A | \chi_{\pm}(\tau) \rangle, \quad (37)$$

$$c'_{\pm}(\tau) = \langle \chi'_{\pm}(\tau) | A | \chi'_{\pm}(\tau) \rangle, \quad (38)$$

and we obtain the correlation function [Eq. (31)]

$$C(t, \tau) = \frac{1}{4} [\mu_{+} \overline{c_{+}(\tau)} - \mu_{-} \overline{c_{-}(\tau)} - i\mu'_{+} \overline{c'_{+}(\tau)} + i\mu'_{-} \overline{c'_{-}(\tau)}]. \quad (39)$$

The averages in Eq. (39) are taken first, for a given $|\phi(t)\rangle$, over the different outcomes for the evolution between 0 and τ of $|\chi_{\pm}(\tau)\rangle$, $|\chi'_{\pm}(\tau)\rangle$, and second, over the different outcomes for the evolution between 0 and t of $|\phi\rangle$ itself.

To prove that this procedure gives the same results as the ones obtained from the master equation and the use of the quantum regression theorem, we consider the quantities κ_{ij} , defined as

$$\begin{aligned} \kappa_{ij}(\tau) = \frac{1}{4} [& \mu_{+} \langle \chi_{+}(\tau) | X_{ij} | \chi_{+}(\tau) \rangle - \mu_{-} \langle \chi_{-}(\tau) | X_{ij} | \chi_{-}(\tau) \rangle \\ & - i\mu'_{+} \langle \chi'_{+}(\tau) | X_{ij} | \chi'_{+}(\tau) \rangle + i\mu'_{-} \langle \chi'_{-}(\tau) | X_{ij} | \chi'_{-}(\tau) \rangle], \end{aligned} \quad (40)$$

and we check that the average $\overline{\kappa_{ij}}$ of these quantities over the different outcomes of the Monte Carlo evolution indeed equals $C_{ij}(t, \tau)$. For $\tau = 0$ this is easily checked from the expressions (35) and (36) for $|\chi_{\pm}(0)\rangle$ and $|\chi'_{\pm}(0)\rangle$:

$$\begin{aligned}
\kappa_{ij}(0) &= \frac{1}{4}[\langle\phi(t)|(1+B^\dagger)X_{ij}(1+B)|\phi(t)\rangle \\
&\quad - \langle\phi(t)|(1-B^\dagger)X_{ij}(1-B)|\phi(t)\rangle \\
&\quad - i\langle\phi(t)|(1-iB^\dagger)X_{ij}(1+iB)|\phi(t)\rangle \\
&\quad + i\langle\phi(t)|(1+B^\dagger)X_{ij}(1-iB)|\phi(t)\rangle] \\
&= \langle\phi(t)|X_{ij}B|\phi(t)\rangle,
\end{aligned} \tag{41}$$

so that

$$\overline{\kappa_{ij}}(0) = C_{ij}(t, 0). \tag{42}$$

Because they are linear combinations of one-time averages and therefore follow from Eq. (34), the evolution of the $\overline{\kappa_{ij}}(\tau)$ values is identical to the evolution of the $C_{ij}(t, \tau)$ values given in Eq. (33). Consequently $\overline{\kappa_{ij}}(\tau)$ coincides with $C_{ij}(t, \tau)$ for any τ .

C. Examples of Correlation Functions

We now consider two examples of the calculation of correlation functions. The first one can be treated completely analytically. It consists in the calculation of the symmetric position correlation function of the damped harmonic oscillator of Eqs. (3) and (5):

$$\begin{aligned}
C_s(t, \tau) &= \langle X(t+\tau)X(t) + X(t)X(t+\tau) \rangle \\
X &= (b + b^\dagger)/\sqrt{2}.
\end{aligned} \tag{43}$$

We note from the derivation of Eq. (41) that, for a Hermitian operator B , the symmetric or antisymmetric correlation functions $\langle A(t+\tau)B(t) \pm B(t)A(t+\tau) \rangle$ can be determined from mean values with only a pair of functions $|\chi_\pm(\tau)\rangle$ or $|\chi'_\pm(\tau)\rangle$. We choose as initial state the ground state of the oscillator $|\phi(0)\rangle = |0\rangle$, which is the steady state of Eq. (3). Therefore $C_s(t, \tau)$ does not depend on t , and the first step of the procedure outlined above, i.e., Monte Carlo evolution of $|\phi\rangle$ between 0 and t is trivial. At time t we construct the two new wave functions $|\chi_\pm(0)\rangle$, which in this simple case give

$$|\chi_\pm(0)\rangle = \sqrt{2/3}|0\rangle \pm (1/\sqrt{3})|1\rangle. \tag{44}$$

We now have to evolve these wave functions and calculate the average values $c_\pm(\tau)$ of X . Fortunately, the stochastic process associated with the evolution of $|\chi_\pm\rangle$ has already been determined. From Eq. (26) we get

$$\begin{aligned}
c_+(\tau) &= -c_-(\tau) = P(\tau)(1/\sqrt{2})[\alpha^*(\tau)\beta(\tau)\exp(-i\omega_0\tau) \\
&\quad + \alpha(\tau)\beta^*(\tau)\exp(i\omega_0\tau)].
\end{aligned} \tag{45}$$

Using Eqs. (24) and (25), we finally obtain

$$C_s(t, \tau) = \cos(\omega_0\tau)\exp(-\Gamma\tau/2), \tag{46}$$

which agrees with the result from the master-equation treatment.³

The second example deals with a laser-driven two-level atom. We suppose here that the laser is strictly resonant so that the atom-laser coupling can be written in the rotating-wave approximation:

$$H_0 = (\hbar\Omega/2)(S^+ + S^-), \tag{47}$$

where Ω is the Rabi frequency characterizing the atom-laser coupling. We want to calculate the dipole correlation function:

$$C(t, \tau) = \langle S^+(t+\tau)S^-(t) \rangle. \tag{48}$$

This calculation is done in steady state so that the Fourier transform of Eq. (48) gives access to the fluorescence spectrum (for a resonant excitation in this case). We proceed in the following way: we start at time $t = 0$ in the ground state, and we let the MCWF evolve for a time sufficiently long to have several quantum jumps (spontaneous emissions). In a density-matrix description this guarantees that the steady state has been reached. In the MCWF approach it implies that there is no memory of initial conditions. From $|\phi(t)\rangle$ obtained in this way we generate n_1 times two pairs of states $|\chi_\pm(\tau)\rangle$ and $|\chi'_\pm(\tau)\rangle$ as defined above, and we calculate the average over those n_1 runs of the quantities (37) and (38). Then we repeat this whole procedure n_2 times, each time getting a new $|\phi(t)\rangle$ from the random evolution of $|\phi\rangle$ between 0 and t . The results of this procedure are indicated in Fig. 1, where we show the values of $C(t, \tau)$ normalized to its value at $\tau = 0$ for various choices of n_1 and n_2 , in comparison with the

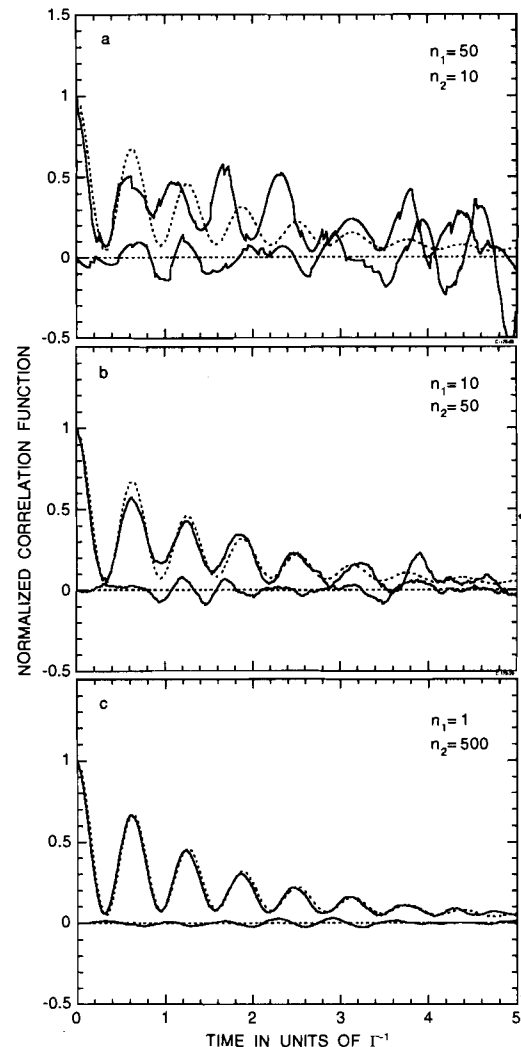


Fig. 1. Solid curves: real part (upper curve) and imaginary part of the dipole correlation function for a two-level atom $\langle S^+(t+\tau)S^-(t) \rangle / \langle S^+(t)S^-(t) \rangle$, for various choices of the numbers n_1 and n_2 (see text). Dotted curves: we have indicated the exact result obtained by using optical Bloch equations and the quantum regression theorem. The field parameters of the calculations are $\Omega = 10\Gamma$, $\delta = 0$.

analytic predictions.²⁸ The same number of $|\chi\rangle$ functions is used in all the calculations. As observed, the higher values of n_2 lead to the best results because they provide a closer description of the state at time t .

5. EXAMPLES

We now give several examples of quantum-optics problems to which the MCWF formalism can be applied. This series of examples is far from being exhaustive, and here we do not intend to give explicit results but simply discuss the main lines of the method in each case.

A. Reservoir at Finite Temperature

We have already discussed the case of a two-level system or of a harmonic oscillator with a spontaneous-emissionlike coupling [Eq. (3)], i.e., a coupling to a bath of harmonic oscillators in its ground state (zero temperature). We can easily extend this treatment to the case of a nonzero-temperature reservoir. In this case we know that the relaxation operator reads as

$$\begin{aligned} \mathcal{L}_{\text{relax}}(\rho_S) = & -(\Gamma/2)[1 + n(\omega_0)] \\ & \times (\sigma^+ \sigma^- \rho_S + \rho_S \sigma^+ \sigma^- - 2\sigma^- \rho_S \sigma^+) \\ & - (\Gamma/2)n(\omega_0)(\sigma^- \sigma^+ \rho_S + \rho_S \sigma^- \sigma^+ - 2\sigma^+ \rho_S \sigma^-), \end{aligned} \quad (49)$$

where σ^\pm are still given by Eqs. (4) and (5) and where $n(\omega_0)$ stands for the mean number of excited quanta at temperature T at the resonance frequency ω_0 of the two-level system or of the oscillator:

$$n(\omega_0) = \left[\exp\left(\frac{\hbar\omega_0}{kT}\right) - 1 \right]^{-1}. \quad (50)$$

By comparison with Eq. (2) we see that in this case we have to deal with two operators C_m :

$$C_1 = \{\Gamma[1 + n(\omega_0)]\}^{1/2} \sigma^-, \quad (51)$$

$$C_2 = [\Gamma n(\omega_0)]^{1/2} \sigma^+. \quad (52)$$

The quantum jumps associated with those two operators correspond to a decay by a spontaneous or a stimulated emission [Eq. (51)] or to an excitation by the absorption of a reservoir quantum of energy [Eq. (52)].

B. Relaxation of Type T_2

We consider here the case of a two-level system, but we now suppose that the relaxation consists of a dephasing between ground- and excited-state amplitudes:

$$\mathcal{L}_{\text{relax}}(\rho_S) = -(1/T_2)(P_e \rho_S P_g + P_g \rho_S P_e) \quad (53)$$

where P_g and P_e denote the projection operators on the ground and the excited states. This relaxation operator damps the nondiagonal terms of the density matrix with a time constant T_2 , but it does not change the populations of the ground or the excited state. In order to treat such a relaxation operator by the MCWF procedure, we rewrite Eq. (53) as

$$\begin{aligned} \mathcal{L}_{\text{relax}}(\rho_S) = & -(1/4T_2)[(P_e - P_g)^2 \rho_S + \rho_S (P_e - P_g)^2] \\ & + (1/2T_2)(P_e - P_g) \rho_S (P_e - P_g). \end{aligned} \quad (54)$$

This has the structure of Eq. (2) with a single C_m operator:

$$C_1 = 1/\sqrt{2T_2}(P_e - P_g). \quad (55)$$

The operator $C_1^\dagger C_1$ is then proportional to identity, and this implies that the wave function remains unchanged when no quantum jump occurs, except for the free evolution that is due to H_S . In a quantum jump the action of the operator C_1 on a wave function $|\phi\rangle = \alpha|g\rangle + \beta|e\rangle$ is simply to change the sign of α and to leave β unchanged. We note also that in this case the probability for a quantum jump δp does not depend on $|\phi\rangle$ since it is always equal to $\delta t/2T_2$.

Let us remark finally that it is quite difficult to associate a measurement process with the quantum jumps resulting from the action of C_1 . A description closer to reality is obtained if we simulate real dephasing collisions of reservoir particles with the system, with each collision having a random duration and a random strength, with mean values leading to relaxation equation (53). The fact that relaxation equation (53) can be brought into the form of Eq. (2), however, implies that such an additional prescription for simulating a wave-function evolution is not required at this point.

C. Spontaneous Emission With Zeeman Degeneracy

We now come back to the problem of spontaneous emission of a two-level system, and we take into account the angular momentum of the ground (J_g) and excited (J_e) levels. In this case we choose a quantization axis z and, in order to give the relaxation equation a simple form in the $|J_g, m_g\rangle_z, |J_e, m_e\rangle_z$ basis, we write it as

$$\begin{aligned} \mathcal{L}_{\text{relax}}(\rho_S) = & -(\Gamma/2)(P_e \rho_S + \rho_S P_e) \\ & + \Gamma \sum_q (\epsilon_q^* \cdot \mathbf{S}^-) \rho_S (\epsilon_q \cdot \mathbf{S}^+), \end{aligned} \quad (56)$$

where ϵ_q is the standard basis associated with the z axis,

$$\epsilon_\pm = \mp 2^{-1/2}(\mathbf{u}_x \pm i\mathbf{u}_y), \quad (57)$$

$$\epsilon_0 = \mathbf{u}_z, \quad (58)$$

and where \mathbf{S}^+ and \mathbf{S}^- are raising and lowering operators proportional to the atomic dipole operator:

$$\begin{aligned} \epsilon_q \cdot \mathbf{S}^+ |J_g, m_g\rangle_z = & (1, J_g, q, m_g; J_e, m_e = m_g + q) \\ & \times |J_e, m_e = m_g + q\rangle_z, \\ \epsilon_q \cdot \mathbf{S}^+ |J_e, m_e\rangle_z = & 0, \\ \epsilon_q^* \cdot \mathbf{S}^- = & (\epsilon_q \cdot \mathbf{S}^+)^\dagger. \end{aligned} \quad (59)$$

In Eqs. (59) a Clebsch-Gordan coefficient enters in the coupling of the ground- and the excited-state sublevels. From Eq. (56) we see that the MCWF procedure will involve three operators C_m :

$$C_q = (\Gamma)^{1/2} (\epsilon_q^* \cdot \mathbf{S}^-), \quad q = 0, \pm 1. \quad (60)$$

We note that the relation

$$\sum_{q=-1}^1 C_q^\dagger C_q = \Gamma \mathbf{S}^+ \cdot \mathbf{S}^- = \Gamma P_e \quad (61)$$

ensures that the relaxation operator (56) has the same structure as Eq. (2). From the measurement point of view presented in Section 3 this corresponds to a simulation in which not only the number of photons emitted dur-

ing δt is detected but also the angular momentum of those photons along a given axis z .

D. Momentum Diffusion in Brownian Motion

We now turn to a problem in which the atomic motion plays a role. We consider the motion of a free particle, with a Hamiltonian H_S given by

$$H_S = P^2/2M. \quad (62)$$

We suppose that this particle interacts with a bath formed by small particles and that this interaction causes a diffusion of the momentum of the Brownian particle with a relaxation operator:

$$\begin{aligned} \mathcal{L}_{\text{relax}}(\rho_S) \\ = -\gamma\rho_S + \gamma \int d^3\mathbf{q} \mathcal{N}(\mathbf{q}) \exp(i\mathbf{q} \cdot \mathbf{R}/\hbar) \rho_S \exp(-i\mathbf{q} \cdot \mathbf{R}/\hbar). \end{aligned} \quad (63)$$

In Eq. (63), \mathbf{R} represents the Brownian particle position operator. The integral is taken over the momentum \mathbf{q} transferred in a collision, and $\mathcal{N}(\mathbf{q})$ is the normalized distribution of those transfers of momentum. The quantity γ is the collision rate.

In the master-equation approach this relaxation equation leads to simple equations of evolution for the populations $\Pi(\mathbf{p})$ of each momentum eigenstate $|\mathbf{p}\rangle$:

$$\dot{\Pi}(\mathbf{p}) = -\gamma\Pi(\mathbf{p}) + \gamma \int d^3\mathbf{q} \mathcal{N}(\mathbf{q}) \Pi(\mathbf{p} - \mathbf{q}). \quad (64)$$

To apply the MCWF formalism, we check that Eq. (63) has the structure of Eq. (2) with an infinity of C_m operators:

$$C_{\mathbf{q}} = [\gamma\mathcal{N}(\mathbf{q})]^{1/2} \exp(i\mathbf{q} \cdot \mathbf{R}/\hbar). \quad (65)$$

This simple form for the C_m values ensures that for an initial state equal to a momentum eigenstate $|\mathbf{p}_0\rangle$, the wave function remains at any time a momentum eigenstate $|\mathbf{p}\rangle$. More precisely, at each step δt there is a probability $1 - \gamma\delta t$ for remaining in this eigenstate and a probability $\gamma\delta t$ for changing \mathbf{p} to $\mathbf{p} + \mathbf{q}$, where \mathbf{q} is determined randomly according to the probability law $\mathcal{N}(\mathbf{q})$. We recover the Monte Carlo simulation that one would perform intuitively by applying to the Brownian particle random kicks with this probability distribution $\mathcal{N}(\mathbf{q})$.

Note that one can also start with a wave function that is a linear superposition of various momentum eigenstates:

$$|\phi(0)\rangle = \sum_i \alpha_i(0) |\mathbf{p}_{i0}\rangle. \quad (66)$$

In this case, $|\phi(t)\rangle$ will remain a superposition of momentum eigenstates $|\mathbf{p}_i\rangle$, which are obtained from the $|\mathbf{p}_{i0}\rangle$ by a translation that is the same for all states. On the other hand, the free evolution of the coefficients $\alpha_i(t)$ that is due to H_S [Eq. (62)] is different for each state. On average, this leads to a damping of the nondiagonal density-matrix elements between the various momentum eigenstates $|\mathbf{p}\rangle$. Such a simulation will reveal the destruction of spatial coherences by the collisions, and it will give access to the spatial diffusion coefficient.

E. Spontaneous Emission Including Recoil

We now come to the description of the center-of-mass motion of an atom that is due to spontaneous emission. With the additional interaction with a laser wave this situation is at the basis of laser cooling and is of great practical importance. The dissipation operator can be written as^{28,30}

$$\begin{aligned} \mathcal{L}_{\text{relax}}(\rho_S) = & -(1/2)(P_e\rho_S + \rho_S P_e) \\ & + (3\Gamma/8\pi) \int d^2\Omega \sum_{\epsilon, \perp \mathbf{k}} \exp(-i\mathbf{k} \cdot \mathbf{R})(\epsilon^* \cdot \mathbf{S}^-) \\ & \times \rho_S(\epsilon \cdot \mathbf{S}^+) \exp(i\mathbf{k} \cdot \mathbf{R}), \end{aligned} \quad (67)$$

where the first line describes the decay of excited-state populations and coherences and of optical coherences by spontaneous emission and the second and third lines describe the corresponding feeding of ground-state populations and coherences. The integral runs over the direction of the emitted photon, with a wave vector \mathbf{k} pointing in the direction of the solid angle Ω , and the sum includes a basis set of two polarizations ϵ orthogonal to this wave vector; \mathbf{R} is the atomic position operator.

We take

$$C_{\Omega, \epsilon} = (3\Gamma/8\pi)^{1/2} \exp(-i\mathbf{k} \cdot \mathbf{R})(\epsilon^* \cdot \mathbf{S}^-), \quad (68)$$

and we check that $\mathcal{L}_{\text{relax}}$ can be put in the form of Eq. (2), with an integral over Ω and a summation over ϵ , by using the following identity:

$$\begin{aligned} \int d^2\Omega \sum_{\epsilon, \perp \mathbf{k}} C_{\Omega, \epsilon}^\dagger C_{\Omega, \epsilon} &= (3\Gamma/8\pi) \int d^2\Omega \sum_{\epsilon, \perp \mathbf{k}} (\epsilon \cdot \mathbf{S}^+) (\epsilon^* \cdot \mathbf{S}^-) \\ &= (3\Gamma/8\pi) \int d^2\Omega (\mathbf{S}^+ \cdot \mathbf{S}^- - [(\mathbf{S}^+ \cdot \mathbf{k}) \\ &\quad \times (\mathbf{S}^- \cdot \mathbf{k})]/k^2) \\ &= \Gamma \mathbf{S}^+ \cdot \mathbf{S}^- = \Gamma P_e. \end{aligned} \quad (69)$$

The probability for getting a quantum jump in the time step δt is given, according to Eq. (69), by $\delta p = \Gamma \Pi_e \delta t$, where Π_e represents the total population of the excited level. When a quantum jump occurs, i.e., when a photon is spontaneously emitted, we make a random choice to determine its direction. This is done by using the normalized probability density for a given direction of emission Ω :

$$\mathcal{P}(\Omega) = \mathcal{P}(\Omega, \epsilon_1) + \mathcal{P}(\Omega, \epsilon_2), \quad (70)$$

where (ϵ_1, ϵ_2) is a polarization basis set orthogonal to the direction Ω and where

$$\mathcal{P}(\Omega, \epsilon_i) = (3/8\pi)(1/\Pi_e) \langle \phi(t) | (\epsilon_i \cdot \mathbf{S}^+) (\epsilon_i^* \cdot \mathbf{S}^-) | \phi(t) \rangle, \quad i = 1, 2. \quad (71)$$

Once the direction of the recoil is known, the polarization ϵ of the photon is chosen between the two possible results ϵ_1, ϵ_2 with the probabilities $\mathcal{P}(\Omega, \epsilon_i)/\mathcal{P}(\Omega)$. Finally, $C_{\Omega, \epsilon}$ is applied to the wave function $|\phi(t)\rangle$ in order to get the state of the system after the quantum jump.

We note that this quite lengthy procedure can be greatly simplified if one restricts it to a simplified spontaneous-emission diagram for which photons are emitted only along a given set of coordinates $\mathbf{u}_x, \mathbf{u}_y, \mathbf{u}_z$. In this case we

can choose also $\mathbf{u}_x, \mathbf{u}_y, \mathbf{u}_z$ as a basis set for the polarization vectors: a photon propagating along \mathbf{u}_x , for instance, can have polarization \mathbf{u}_y or \mathbf{u}_z . This leads to a replacement of the integral over Ω in Eq. (67) by a sum of only six terms $\mathbf{k} = \pm \hbar \mathbf{u}_i$:

$$(\Gamma/2) \sum_{\mathbf{e}=\mathbf{u}_x, \mathbf{u}_y, \mathbf{u}_z} \sum_{\mathbf{k} \perp \mathbf{e}} \exp(-i\mathbf{k} \cdot \mathbf{R}) \times (\mathbf{e} \cdot \mathbf{S}^-) \rho_S (\mathbf{e} \cdot \mathbf{S}^+) \exp(i\mathbf{k} \cdot \mathbf{R}). \quad (72)$$

When one is not interested in the detailed effect of the spontaneous-emission pattern on the atomic dynamics, this approximation brings a significant simplification to the MCWF procedure.

Another simplification occurs when only the atomic motion in one dimension, for example, along the z axis, is considered, as is the case, for example, in one-dimensional laser cooling calculations. We then take the trace of Eq. (67) over the x and y variables, which leaves us with the relaxation equation^{29,31}

$$\begin{aligned} \mathcal{L}_{\text{relax}}(\rho_S) = & -(\Gamma/2)(P_z \rho_S + \rho_S P_z) \\ & + \Gamma \sum_{q=-1}^1 \int_{-k}^k dk' N_q(k') \exp(-ik'Z) (\mathbf{e}_q^* \cdot \mathbf{S}^-) \\ & \times \rho_S (\mathbf{e}_q \cdot \mathbf{S}^+) \exp(ik'Z). \end{aligned} \quad (73)$$

The vectors \mathbf{e}_q have been introduced in Eqs. (57) and (58), and $N_q(k')$ is the normalized probability density for having a spontaneous photon with angular momentum $\hbar q$ and linear momentum $\hbar k'$ along the z axis:

$$N_{\pm 1}(k') = (3/8k) \left[1 + \left(\frac{k'}{k} \right)^2 \right], \quad (74)$$

$$N_0(k') = (3/4k) \left[1 - \left(\frac{k'}{k} \right)^2 \right]. \quad (75)$$

The Monte Carlo procedure corresponds in this case to the detection of the momentum $\hbar k'$ of the emitted photon along the z axis and of the angular momentum of the photon along the same axis. The corresponding C_m operators are

$$C_{k',q} = [\Gamma N_q(k')]^{1/2} \exp(-ik'Z) (\mathbf{e}^* \cdot \mathbf{S}^-). \quad (76)$$

We use this form in Subsection 5.F, which is devoted to Doppler cooling.

F. Doppler Cooling

We now focus on the case of one-dimensional Doppler cooling of a two-level atom, for which we present some numerical results. This will give an illustration of the effectiveness of the MCWF method as compared with the master-equation approach when the number of states is not too low.

1. The Model

An atom with a transition $J_g \leftrightarrow J_e = J_g + 1$ is placed in a σ_+ polarized standing wave so that only the Zeeman sublevels $|g, m_g = J_g\rangle$ and $|e, m_e = J_e\rangle$ play a role; for simplicity we denote these substates as $|g\rangle$ and $|e\rangle$ in what follows. Doppler cooling occurs for negative values of the detuning

$\delta = \omega_L - \omega_A$ between the laser and the atomic frequencies; it originates from the fact that a moving atom is closer to resonance with the counterpropagating component of the wave than with the copropagating one; the atom therefore feels a net radiation pressure force opposed to its velocity.^{32,33} This picture works well at non-saturating laser intensities, where one can add the effect of the two waves independently. At higher intensities this type of semi-classical analysis based on the calculation of a damping force becomes more complicated,^{34,35} and a quantum treatment of the atomic external motion is a good alternative. Here we present the result of such an analysis using both a master-equation and a MCWF approach.

The Hamiltonian H_S using the rotating wave approximation reads as²⁵

$$H_S = (P^2/2M) + \hbar \Omega \cos(kZ)(S^+ + S^-) - \hbar \delta P_z, \quad (77)$$

where Z and P are the atomic position and momentum operators and Ω is the Rabi frequency of each traveling wave forming the standing wave. We choose the initial wave function $|\phi(0)\rangle$ equal to $|g, p = 0\rangle$. At a time t , $|\phi(t)\rangle$ can be written as

$$\begin{aligned} |\phi(t)\rangle = & \sum_n \alpha_n(t) |g, p = p_0 + 2n\hbar k\rangle \\ & + \beta_n(t) |e, p = p_0 + (2n + 1)\hbar k\rangle, \end{aligned} \quad (78)$$

where the momentum p_0 depends on the random recoils that have occurred between 0 and t and remains constant between two quantum jumps. According to Subsection 2.B, evolution of α_n and β_n consists of sequences of two steps. First, the wave function evolves linearly with the non-Hermitian Hamiltonian $H = H_S - i\hbar \Gamma P_z/2$:

$$i\dot{\alpha}_n = \frac{(p_0 + 2n\hbar k)^2}{2M\hbar} \alpha_n + \frac{\Omega}{2} (\beta_n + \beta_{n-1}), \quad (79)$$

$$\begin{aligned} i\dot{\beta}_n = & \left\{ \frac{[p_0 + (2n + 1)\hbar k]^2}{2M\hbar} - \delta - \frac{i\Gamma}{2} \right\} \beta_n \\ & + \frac{\Omega}{2} (\alpha_n + \alpha_{n+1}). \end{aligned} \quad (80)$$

Then we randomly decide whether a quantum jump occurs. The probability δp for a jump is proportional to the total excited-state population:

$$\delta p = \Gamma \sum_n |\beta_n|^2 \delta t. \quad (81)$$

If no quantum jump occurs, we simply normalize the wave function. If a quantum jump occurs, the momentum $\hbar k'$ along the z axis of the fluorescence photon is chosen randomly with the probability law $N_+(k')$ [Eq. (74)], and the new wave function is obtained by the action of

$$C_{k'} = [\Gamma N_+(k')]^{1/2} \exp(-ik'Z) S^- \quad (82)$$

on $|\phi(t)\rangle$. This leads to

$$\alpha_n(t + \delta t) = \mu \beta_n(t), \quad (83)$$

$$\beta_n(t + \delta t) = 0, \quad (84)$$

$$p_0 \rightarrow p_0 + \hbar k - \hbar k', \quad (85)$$

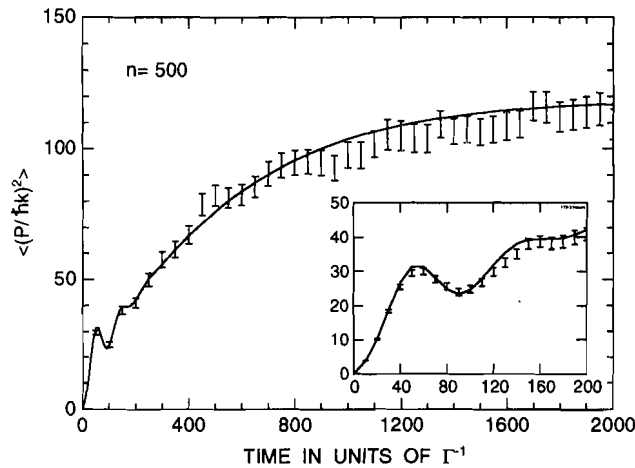


Fig. 2. Time evolution of $\langle P^2 \rangle$ in Doppler cooling. Time is measured in units of the excited-state lifetime Γ^{-1} , and momentum in units of $\hbar k$. The detuning δ and the Rabi frequency Ω are given by $\Omega = -\delta = \Gamma/2$. The atomic mass is such that $\Gamma = 200\hbar k^2/M$. The points represent the Monte Carlo results, obtained by averaging $n = 500$ MCWF evolutions. The error bars correspond to the statistical error $\delta P^2_{(n)}$. We have also indicated by a curve the results of the density-matrix approach. Both calculations involve 200 quantum levels and take approximately the same computing time on a scalar machine. In the inset we have detailed the short-time regime corresponding to the diffraction of the atomic de Broglie wave by the laser standing wave.

where μ is a normalization coefficient. We note that in this way the recoil that is due to spontaneous emission is treated in an exact manner. In the master-equation approach an exact treatment of the spontaneous recoil requires a discretization of atomic momenta on a grid with a step size smaller than $\hbar k$. This increases the amount of calculation of the master equation with respect to the MCWF one, in addition to the N -versus- N^2 argument mentioned in Section 1.

In order to make a fair comparison between the two approaches, we have chosen a coarse discretization for the atomic momentum, with a step size $\hbar k$, i.e., $k' = -k, 0$, or k . An optimum representation of the diffusion rate that is due to the directional distribution of spontaneously emitted photons is obtained by taking the probability law for the quantum jumps governed by C_{-k}, C_0, C_k to be $1/2:3/5:1/5$. The corresponding modified values of $N_+(k')$ are then also used in the master-equation calculations for this problem.

2. Numerical Results

We have considered the case of sodium atoms ($\Gamma = 200 \hbar k^2/M$), for which the minimal Doppler cooling limit, obtained for $\delta = -\Gamma/2$ and $\Omega \ll \Gamma$, corresponds to $p_{rms} = 8.4 \hbar k$. We have discretized the momentum between $-50 \hbar k$ and $+50 \hbar k$, which corresponds to a basis with 202 eigenstates total, with at any time 101 nonzero coefficients α_n and β_n [see Eq. (78), where p_0 is either an odd or an even multiple of $\hbar k$].

The results for the evolution of the sample mean $\langle P^2 \rangle_{(n)}$, defined as

$$\langle P^2 \rangle_{(n)}(t) = \frac{1}{n} \sum_{i=1}^n \langle \phi^{(i)}(t) | P^2 | \phi^{(i)}(t) \rangle, \quad (86)$$

are given in Fig. 2, together with the results for $\langle P^2 \rangle(t)$ obtained by using the master-equation treatment. These

results correspond to the parameters $\Omega = -\delta = \Gamma/2$. The MCWF results have been obtained with the average of $n = 500$ evolutions.

In Fig. 2 we have indicated the statistical error $\delta P^2_{(n)}$ on the determination of $\langle P^2 \rangle_{(n)}$. This quantity $\delta P^2_{(n)}$, which is defined in Section 7, gives an estimate of the quality of the result, and with $n = 500$ wave functions the signal-to-noise ratio in the range of 20 is quite satisfactory.

With a scalar machine we have found that the time required for the calculation with 500 wave functions is equal to the time required for the master-equation evolution. With a vectorial compiler we have found that there is an additional gain of a factor 15 in the benefit of the MCWF procedure. Therefore, even for this relatively simple one-dimensional problem with only 200 levels, the MCWF method is at least as efficient as the master-equation approach for determining cooling limits with a good precision.

In Fig. 2 we clearly see the existence of two regimes in the evolution of $\langle P^2 \rangle(t)$. For short times ($t < 200\Gamma^{-1}$; see the inset of Fig. 2) the number of spontaneous emissions is small, and the physics involved is essentially the diffraction of the plane atomic de Broglie wave by the grating formed by the laser standing wave.³⁶ For longer interaction times, dissipation comes into play^{37,38} and $\langle P^2 \rangle(t)$ tends to a steady-state value, of the order of $(11\hbar k)^2$. This value for p_{rms} is larger than the Doppler cooling limit ($8.4 \hbar k$) because of saturation effects.

Figure 3 shows the evolution of the momentum distribution of a single MCWF. The MCWF extends over approximately $5\hbar k$ and explores as time goes on all the significant parts of the momentum space. In Fig. 4 we have given the evolution of the momentum distributions obtained by the master-equation approach (Fig. 4a) and by the MCWF approach after average (Fig. 4b). In Section 7 we will compare the convergence of the MCWF method for global operators (i.e., P^2) and for local operators (i.e., population of a single state).

6. EQUIVALENT MONTE CARLO SIMULATIONS FOR A GIVEN MASTER EQUATION

In this section we discuss the existence of several different Monte Carlo approaches for a given relaxation opera-

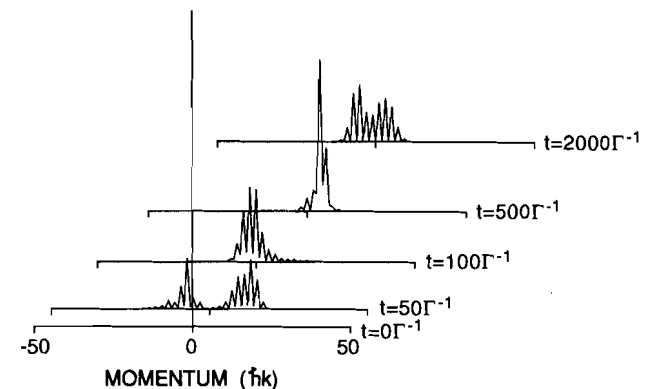


Fig. 3. Time evolution of the momentum distribution for a single Monte Carlo wave function for the Doppler cooling situation described in Fig. 2. The MCWF extends over approximately $5\hbar k$ and explores as time goes on all significant parts of the momentum space.

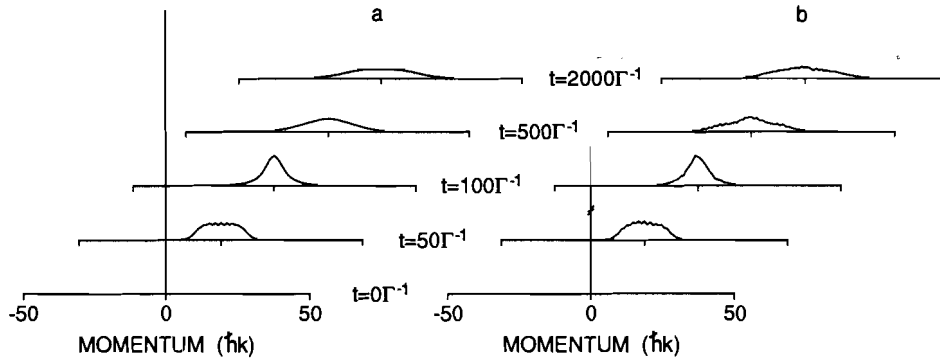


Fig. 4. Time evolution of the atomic momentum distributions, obtained for the Doppler cooling situation described in Fig. 2. a, Result of the master-equation approach. b, Result of the average of 500 MCWF's.

for $\mathcal{L}_{\text{relax}}$, leading in average to the same results but with possibly different physical pictures.

Here we restrict ourselves to the class of Monte Carlo approaches that are related by a given invariance property of the relaxation operator $\mathcal{L}_{\text{relax}}$. Suppose that there exists an operator T , acting in the Hilbert space of the system, such that

$$T[\mathcal{L}_{\text{relax}}(\rho_S)]T^\dagger = \mathcal{L}_{\text{relax}}(T\rho_S T^\dagger). \quad (87)$$

This operator T can be, for instance, a rotation operator, and Eq. (87) is then fulfilled if the dissipation process is isotropic. Equation (87) can be transformed into

$$\mathcal{L}_{\text{relax}}(\rho_S) = T^\dagger \mathcal{L}_{\text{relax}}(T\rho_S T^\dagger)T, \quad (88)$$

which means that we can write the relaxation operator alternatively as

$$\begin{aligned} \mathcal{L}_{\text{relax}}(\rho_S) = & -\frac{1}{2} \sum_m (D_m^\dagger D_m \rho_S + \rho_S D_m^\dagger D_m) \\ & + \sum_m D_m \rho_S D_m^\dagger, \end{aligned} \quad (89)$$

with

$$D_m = T^\dagger C_m T. \quad (90)$$

We can therefore perform the Monte Carlo simulation either with the set of operators C_m or with the set of operators D_m . The physical pictures given by these two Monte Carlo simulations may be quite different from each other, although we know that their predictions concerning one-time averages or two-time correlation functions are the same. The choice of a particular simulation should be made by considering the convergence of the numerical calculation, as we show in Section 7, or for emphasizing a particular physical aspect of the problem.

We now give an example of two equivalent Monte Carlo simulations for the same physical process. Consider a $g, J_g = 1 \leftrightarrow e, J_e = 1$ transition irradiated by two resonant laser fields with the same intensity and polarized σ_+ and σ_- with respect to the z axis (Fig. 5a). It is known from the analysis by optical Bloch equations that the atomic population is eventually trapped in a ground state that is not coupled to the laser field. This is related to the dark resonance phenomenon. If we suppose that the two waves are in phase, this dark state is

$$|\phi_{\text{NC}}\rangle = (|g, m_z = -1\rangle + |g, m_z = 1\rangle)/\sqrt{2}. \quad (91)$$

The first MCWF analysis can be done by using the operators C_q defined in Eq. (60), obtained after writing the relaxation equation with z as quantization axis. Suppose that the atom starts, for instance, in $|g, m_z = -1\rangle$. The atom-laser coupling leads first to an increase of the population of the excited state $|e, m_z = 0\rangle$. A spontaneous photon may then be emitted (Fig. 6a), which, depending on its angular momentum $q_z = \pm 1$, puts the atom back into $|g, m_z = \mp 1\rangle$ (the transition $|e, m_z = 0\rangle \rightarrow |g, m_z = 0\rangle$ is forbidden because of the vanishing Clebsch-Gordan coefficient). However, it may also happen that no spontaneous photon is detected after a long time, with the successive steps of evolution owing to the non-Hermitian Hamiltonian H and renormalization of the resulting wave function causing a continuous rotation from $|g, m_z = \pm 1\rangle$ into $|\phi_{\text{NC}}\rangle$ and therefore trapping the atomic population into this state (last part of the time sequence of Fig. 6a).

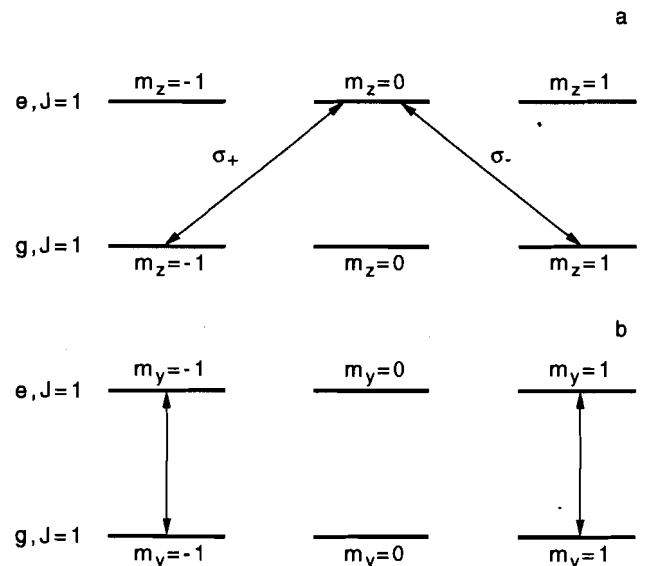


Fig. 5. Configuration schemes leading to a dark resonance: a, $g, J_g = 1 \leftrightarrow e, J_e = 1$ transition is irradiated by two waves respectively σ_+ and σ_- polarized along the z axis. a, If angular momentum is quantized along the z axis, the dark resonance appears as the formation of a nonabsorbing state, which is a linear combination of $|g, m_z = -1\rangle$ and $|g, m_z = 1\rangle$. b, If angular momentum is quantized along the axis parallel with the resulting linear polarization of the light (y axis), the dark resonance corresponds to an optical pumping to the $|g, m_y = 0\rangle$ state, which is not coupled to the light because the Clebsch-Gordan coefficient connecting $|g, J_g = 1, m_y = 0\rangle$ and $|e, J_e = 1, m_y = 0\rangle$ is zero.

Note that the continuous rotation into the trapping state is of the same type as the one seen in Section 3 for the spontaneous emission of an oscillator in a linear superposition of the ground and the excited state.

Now we can replace the set of operators C_q by a different set obtained in choosing a different quantization axis. For instance, suppose that we choose this new quantization axis y parallel to the resulting linear polarization of the laser light at the atom position. Because of the π polarization of the laser excitation along that axis (see Fig. 5b) we now identify the trapping state as

$$|\phi_{NC}\rangle = |g, m_y = 0\rangle, \quad (92)$$

and we perform the Monte Carlo simulation by using the set of operators D_q that are analogous to those given in Eq. (60) but defined now with respect to the y axis. In Fig. 6b we have plotted such a simulation involving two quantum jumps. We start again in the state $|g, m_z = -1\rangle$ that we expand on the $|g, m_y\rangle$ basis. In the first part of the evolution a continuous rotation toward $|g, m_y = 0\rangle$ takes place. Then a first photon with $q_y = 0$ is detected; this detection projects the wave function onto a superposition of $|g, m_y = \pm 1\rangle$ and the population of the trapping state $|g, m_y = 0\rangle$ is 0. The atom then cycles between $|g, m_y = \pm 1\rangle$ and $|e, m_y = \pm 1\rangle$, and the population of the trapping state remains zero until one detects a second photon with a polarization $q_y = \pm 1$. This detection projects the wave function into the trapping state. The way the system enters into the dark resonance is then more readily understood as a kind of optical pumping.

In Figs. 6c and 6d we check that the two simulations lead to the same average results. We observe smaller fluctuations in the results obtained with the quantization along the z axis; the reason for this difference in the quality of the simulation is explained in Section 7.

7. GETTING GOOD STATISTICS WITH THE MONTE CARLO WAVE-FUNCTION METHOD

A. Definition of a Signal-to-Noise Ratio

A primary goal of our procedure is to determine the average value $\langle A \rangle(t)$ at time t of a given Hermitian system operator A , knowing the state of the system at time 0. Applying our MCWF method with a number n of simulations, we obtain the sample mean

$$\langle A \rangle_{(n)}(t) = \frac{1}{n} \sum_{i=1}^n \langle \phi^{(i)}(t) | A | \phi^{(i)}(t) \rangle, \quad (93)$$

which will approximate $\langle A \rangle(t)$ with a statistical error $\delta A_{(n)}$ related to the square root of the sample variance $(\Delta A)_{(n)}^2$ by

$$\delta A_{(n)} = \Delta A_{(n)} / \sqrt{n}, \quad (94)$$

with³⁹

$$(\Delta A)_{(n)}^2(t) = \frac{1}{n} \left(\sum_{i=1}^n \langle \phi^{(i)}(t) | A | \phi^{(i)}(t) \rangle^2 \right) - \langle A \rangle_{(n)}^2(t). \quad (95)$$

When n is large compared with 1, the sample variance tends to a finite value that we denote $\Delta A_{(\infty)}^2$. Consequently, the condition for having a good signal-to-noise ratio $\langle A \rangle / \delta A_{(n)}$ can be written as [if $\langle A \rangle(t)$ is expected to be zero, it may be replaced by the precision that one requires

for the calculation]

$$\sqrt{n} \gg \Delta A_{(\infty)}(t) / [\langle A \rangle(t)]. \quad (96)$$

In the following we give an estimate of $(\Delta A)_{(\infty)}^2(t)$, and we then discuss the requirement on n given by the inequality (96) in terms of *local* or *global* operators.

B. Estimate of the Sample Variance

To estimate $(\Delta A)_{(\infty)}^2(t)$, we use the general inequality

$$\langle \phi | A | \phi \rangle^2 \leq \langle \phi | A^2 | \phi \rangle. \quad (97)$$

Expression (95) can be overestimated by

$$(\Delta A)_{(n)}^2(t) \leq \frac{1}{n} \left(\sum_{i=1}^n \langle \phi^{(i)}(t) | A^2 | \phi^{(i)}(t) \rangle \right) - \langle A \rangle_{(n)}^2(t). \quad (98)$$

When n is large compared with 1, the two terms of the right-hand side of this expression have a finite limit. The first term tends to $\langle A^2 \rangle(t)$, and the second tends to $\langle A \rangle^2(t)$, where the averages are now taken in the system density matrix at time t . The right-hand side of inequality (98) therefore tends to the variance $(\Delta A)_{(\rho_S)}^2(t)$ of the operator A for a system in a state described by the density matrix $\rho_S(t)$:

$$(\Delta A)_{(\rho_S)}^2(t) = \text{Tr}[\rho_S(t) A^2] - [\text{Tr}(\rho_S A)]^2. \quad (99)$$

We therefore have the following overestimate of $(\Delta A)_{(\infty)}^2(t)$:

$$(\Delta A)_{(\infty)}^2(t) \leq (\Delta A)_{(\rho_S)}^2(t). \quad (100)$$

Consequently, a sufficient condition on n deduced from inequality (96) is

$$\sqrt{n} \gg \Delta A_{(\rho_S)}(t) / [\langle A \rangle(t)]. \quad (101)$$

We note that inequality (100) becomes an identity if all the $|\phi^{(i)}(t)\rangle$ are eigenstates of the operator A . This is the case for instance in the study of Brownian motion outlined in Subsection 5.D, if we take $|\phi(t)\rangle = |\mathbf{p}\rangle$ and if we choose A

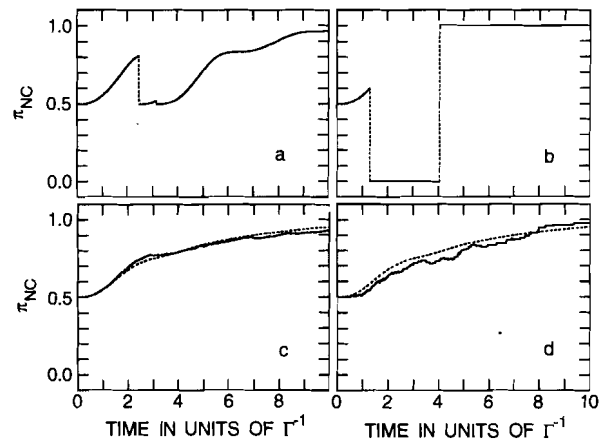


Fig. 6. MCWF simulation of a dark resonance. The population of the uncoupled state in a single MCWF evolution, corresponding to a measurement of the photon angular momentum along the z axis, a, or along the y axis, b. The two types of evolution are clearly different. Average of 100 MCWF evolutions, with a measurement of the photon angular momentum along the z axis, c, or along the y axis, d. Apart from fluctuations, the two simulations lead to the same result, as expected.

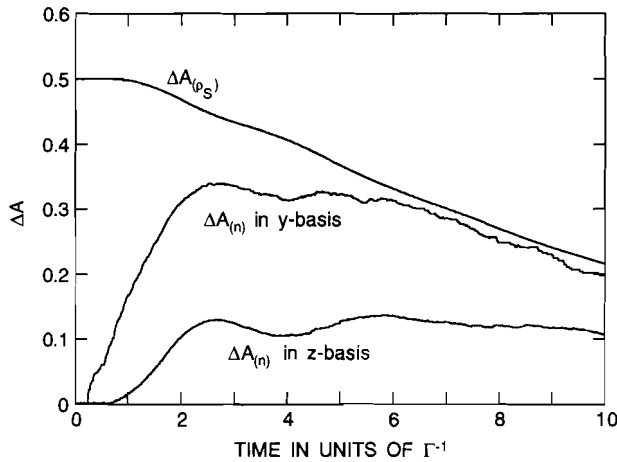


Fig. 7. Time evolution of the variance $\Delta A_{(\rho_S)}(t)$ and of the sample variances $\Delta A_{(n)}(t)$ obtained for the two simulations with the y and z quantization axis for the dark resonance problem ($n = 1000$). The sample variance for the y axis choice is close to its upper bound $\Delta A_{(\rho_S)}(t)$, whereas the simulation with the choice of the z axis leads to a noise that is more than two times smaller (also compare Figs. 6c and 6d).

equal to the projection operator on a given $|\mathbf{p}_0\rangle$: $A = |\mathbf{p}_0\rangle\langle\mathbf{p}_0|$. For the case of Doppler cooling, taking $A = P^2$, we have found in steady state that $\Delta A_{(n)} \approx 0.8\Delta A_{(\rho_S)}$ for $n = 500$; the difference between these two quantities is essentially determined by the typical width of the individual MCWF's (cf. Fig. 3).

Let us also emphasize that, in contrast to $\Delta A_{(\rho_S)}(t)$, the quantity $\Delta A_{(\infty)}(t)$ can vary for a given system with the choice of the set of the C_m operators. We illustrate this point for the example of dark resonances discussed at the end of the previous section. We choose $A = |\phi_{NC}\rangle\langle\phi_{NC}|$, whose average value gives the population of the trapping state, and in Fig. 7 we plot the value of $\Delta A_{(\rho_S)}(t)$ and of the $\Delta A_{(n)}(t)$ values obtained for the two simulations with the y and z quantization axes. The initial state is $|g, m_z = -1\rangle$ for the three curves. We have taken $n = 1000$ so that $\Delta A_{(n)}(t) \approx \Delta A_{(\infty)}(t)$. In Fig. 7 one clearly sees that inequality (100) is confirmed for this example. We also note that the simulation with the y quantization axis has a $\Delta A_{(\infty)}$ close to its upper bound; this is easily understood since in this case, as soon as one quantum jump occurs, the wave function is in an eigenstate of A , with the eigenvalue 0 if the detected photon is π polarized or 1 if it is σ_{\pm} polarized. The simulation with quantization along the z axis leads to $\Delta A_{(n)}(t)$ smaller by a factor of 2 and is therefore more appropriate if one looks for a rapidly converging procedure.

C. Local versus Global Operators

In order to discuss the requirements imposed by inequality (101), we now split the various operators A into two kinds. First, there are local operators, such as the ones giving the population of a particular state $|j\rangle$, $A = |j\rangle\langle j|$ and $A^2 = A$. For those operators we expect that

$$\langle A \rangle(t) \sim \frac{1}{N}, \quad (\Delta A)_{(\rho_S)}^2(t) \sim \frac{1}{N}, \quad (102)$$

where N denotes the total number of quantum levels involved in the simulation (we suppose here that $N \gg 1$).

If we insert these values into inequality (101), we see that the number n of simulations that have to be performed must be larger than the number of levels N :

$$\text{local operators} \quad n \gg N. \quad (103)$$

Clearly one does not gain by using a Monte Carlo treatment in this case. The amount of calculation for determining a single $|\phi(t)\rangle$ is reduced by a factor N with respect to the calculation of the density matrix $\rho_S(t)$, but one has to repeat n MCWF runs to get good statistics, with $n > N$.

We note that inequality (100) is in fact an overestimate of $\Delta A_{(\infty)}$ and that wave functions extending over several eigenstates of the operator A of interest lead to smaller values of $\Delta A_{(\infty)}$ compared with $\Delta A_{(\rho_S)}$. This may in particular be the case for the local operators, and the typical momentum width of a Monte Carlo wave function in our simulation of laser cooling (see Fig. 3) leads to a much better agreement between the momentum distributions in Fig. 4a and 4b than expected from relations (101) and (102). To illustrate this, we calculated the fluctuations in the population of the zero-momentum state, described by the local operator $A = |p=0\rangle\langle p=0|$; we obtained at time $t = 2000\Gamma^{-1}$ the values $\langle A \rangle_{(n)} = 4 \times 10^{-2}$, $(\Delta A)_{(n)}^2 = 7 \times 10^{-3}$. The ratio between these quantities is proportional to the typical width in momentum space of a wave function and weakens constraint (103), which was deduced from relations (101) and (102).

The MCWF treatment is more efficient if one deals with global operators, such as the population of a large group of levels, or, for the description of laser cooling, the average kinetic energy. For those operators we have

$$\Delta A_{(\rho_S)}(t) \sim \langle A \rangle(t). \quad (104)$$

For instance, if we consider the problem of a Brownian particle thermalized with a reservoir at temperature T and if we take $A = P^2/2M$, we get in steady state

$$\langle A \rangle = (3/2)k_B T, \quad \Delta A_{(\rho_S)} = \sqrt{3/2}k_B T. \quad (105)$$

In this case we see from inequality (101) that good statistics are obtained after n Monte Carlo runs as soon as

$$\text{global operators} \quad n \gg 1. \quad (106)$$

If one requires, say, a 10% accuracy for the average of global operators, inequality (106) dictates the choice $n \approx 100$. Thus, when the number N of levels involved is larger than this number, the MCWF treatment may be more efficient than the master-equation approach. To compare with laser cooling experiments, a 10% accuracy will usually be sufficient, and even for the simple case of Doppler cooling we have noted that the stochastic evolution of wave functions is competitive with the integration of the density-matrix equation.

8. CONCLUSION

As we mentioned in the Introduction, there have recently been a number of papers that discuss the applicability of stochastic methods as an alternative to the usual treatment of master equations in quantum mechanics. These may draw on different sources of inspiration, but they all lead to a description involving a stochastic wave-function

evolution, which may be either continuous¹² or involve quantum jumps.^{6,7,10,11}

In the present paper we have presented a stochastic evolution for the wave function of a system coupled to a reservoir generalizing that of Ref. 6. We have proved the equivalence of this Monte Carlo wave-function approach with the master-equation treatment, and we have given several examples where it can be applied. In addition, we have considered in detail the efficiency with which expectation values of physical observables may be calculated with this method. In order to control the fluctuations inherent in any simulation procedure, one must propagate a large number of wave functions and, depending on the dimensionality of the system Hilbert space and on the type of observable considered, the simulations may be more or less efficient than the master-equation treatment.

As an example, we considered one-dimensional laser cooling of two state atoms, and these calculations bring promises for our present attempts to treat more general three-dimensional cooling. Also, a method for calculating two-time correlation functions was demonstrated; the applicability of this method to the more complex problem of the spectrum from cooled atoms in optical molasses is now being studied (see also Ref. 41).

Apart from a numerical procedure, the replacement of the density matrix by wave functions provides new insight; for example, it reveals mechanisms for the evolution of the system that may manifest themselves less clearly in the master-equation approach. We wish to emphasize, however, that by the MCWF procedure one does not get knowledge of how individual systems in an ensemble actually evolve and how they contribute to the averages as obtained by the density matrix. At the level of individual wave functions the method only provides a model. As we saw in Section 6, several different such models can apply, and none of these models can be claimed to yield a more typical realization than the others. It is noteworthy, though, that if a particular detection scheme is invoked, according to our measurement interpretation of the MCWF procedure, the Monte Carlo wave function does correspond to a true evolution of the system according to standard quantum mechanics.

As seen from another perspective, this work confronts two very different definitions of the density matrix: (i) a reduction, by means of a trace, of the state of the combined system + reservoir, which can no longer be described by a pure state in the small system, and (ii) a statistical description of an ensemble of systems populating different states with a given probability law. Which of the two underlying interpretations for the density matrix is used has no influence on the way in which mean values are obtained; this explains why the master equation, which is certainly derived from the first definition for the density matrix, can be treated by our MCWF method, which relies on the second interpretation.

ACKNOWLEDGMENTS

We are grateful to C. Cohen-Tannoudji, A. Aspect, C. Salomon, W. D. Phillips, P. D. Lett, and K. Berg-Sørensen for many helpful discussions. The Laboratoire de Spectroscopie Hertzienne is a Unité de Recherche de l'Ecole Normale Supérieure et de l'Université Paris 6

and is associated with the Centre National de la Recherche Scientifique.

REFERENCES AND NOTES

1. W. H. Louisell, *Quantum Statistical Properties of Radiation* (Wiley, New York, 1973).
2. F. Haake, *Statistical Treatment of Open Systems by Generalized Master Equations*, G. Hohler, ed., Vol. 66 of Springer Tracts in Modern Physics (Springer-Verlag, Berlin, 1973).
3. C. Cohen-Tannoudji, in *Les Houches 1975, Frontiers in Laser Spectroscopy*, R. Balian, S. Haroche, and S. Liberman, eds. (North-Holland, Amsterdam, 1977).
4. C. W. Gardiner, *Handbook of Stochastic Methods* (Springer-Verlag, Berlin, 1983).
5. M. Lax, *Phys. Rev.* **172**, 350 (1968).
6. J. Dalibard, Y. Castin, and K. Mølmer, *Phys. Rev. Lett.* **68**, 580 (1992).
7. H. J. Carmichael, "An open systems approach to quantum optics," lectures presented at l'Université Libre de Bruxelles, Bruxelles, Belgium, fall 1991.
8. P. L. Kelley and W. H. Kleiner, *Phys. Rev.* **136**, A316 (1964).
9. M. D. Srinivas and E. B. Davies, *Opt. Acta* **28**, 981 (1981).
10. R. Dum, P. Zoller, and H. Ritsch, *Phys. Rev. A* **45**, 4879 (1992).
11. G. C. Hegerfeldt and T. S. Wilser, in *Proceedings of the II International Wigner Symposium, July 1991, Goslar* (World Scientific, Singapore, to be published).
12. N. Gisin, *Phys. Rev. Lett.* **52**, 1657 (1984); *Helvetica Phys. Acta* **62**, 363 (1989).
13. B. Misra and E. C. G. Sudarshan, *J. Math. Phys.* **18**, 756 (1977).
14. R. H. Dicke, *Am. J. Phys.* **49**, 925 (1981).
15. D. T. Pegg and P. L. Knight, *Phys. Rev. A* **37**, 4303 (1988).
16. R. J. Cook, in *Progress in Optics XXVIII*, E. Wolf, ed., (Elsevier, New York, 1990), p. 363.
17. M. Porrati and S. Putterman, *Phys. Rev. A* **36**, 929 (1987).
18. R. Mollow, *Phys. Rev. A* **12**, 1919 (1975).
19. C. Cohen-Tannoudji and J. Dalibard, *Europhys. Lett.* **1**, 441 (1986).
20. P. Zoller, M. Marte, and D. F. Walls, *Phys. Rev. A* **35**, 198 (1987).
21. H. J. Carmichael, S. Singh, R. Vyas, and P. R. Rice, *Phys. Rev. A* **39**, 1200 (1989).
22. R. Blatt, W. Ertmer, P. Zoller, and J. L. Hall, *Phys. Rev. A* **34**, 3022 (1986).
23. C. Cohen-Tannoudji, F. Bardou, and A. Aspect, in *Laser Spectroscopy*, X. M. Duclouy, E. Giacobino, and G. Camy, eds. (World Scientific, Singapore, to be published).
24. C. Cohen-Tannoudji, B. Zambon, and E. Arimondo, *C. R. Acad. Sci. Paris* **314**, 1139 (1992); **314**, 1293 (1992).
25. V. P. Belavkin and P. Staszewski, *Phys. Rev. A* **45**, 1347 (1992).
26. N. Gisin, Group of Applied Physics, University of Geneva, 1211 Geneva 4, Switzerland (personal communication); N. Gisin and I. Percival, *Phys. Rev. A* **46**, 4382 (1992).
27. A different procedure for calculating spectra has been recently proposed by R. Dum, A. S. Parkins, P. Zoller, and C. W. Gardiner, *Phys. Rev. A* **46**, 4382 (1992). It is based on the probing of the atomic system with either a monochromatic weak laser or a white noise driving field.
28. R. Loudon, *The Quantum Theory of Light* (Oxford U. Press, New York, 1983).
29. J. Javanainen and S. Stenholm, *Appl. Phys.* **21**, 35 (1980).
30. C. Cohen-Tannoudji, in *Les Houches 1990, Fundamental Systems in Quantum Optics*, J. Dalibard, J.-M. Raimond, and J. Zinn-Justin, eds. (North-Holland, Amsterdam, 1992).
31. Y. Castin, H. Wallis, and J. Dalibard, *J. Opt. Soc. Am. B* **6**, 2046 (1989).
32. T. W. Hänsch and A. Schawlow, *Opt. Commun.* **13**, 68 (1975).
33. D. Wineland and H. Dehmelt, *Bull. Am. Phys. Soc.* **20**, 637 (1975).
34. V. G. Minogin, *Sov. Phys. JETP* **53**, 1164 (1981).
35. K. Berg-Sørensen, E. Bonderup, K. Mølmer, and Y. Castin, *J. Phys. B* **25**, 4195 (1992).

36. C. Tanguy, S. Reynaud, and C. Cohen-Tannoudji, *J. Phys. B* **17**, 4623 (1984).
37. M. Wilkens, E. Schumacher, and P. Meystre, *Opt. Commun.* **86**, 34 (1991).
38. S. Stenholm in *Laser Manipulation of Atoms and Ions*, E. Arimondo and W. D. Phillips, eds. (North-Holland, Amsterdam, 1992).
39. Strictly speaking, we should put $1/(n - 1)$ instead of $1/n$ as a normalization factor; see S. Brandt, *Statistical and Computational Methods in Data Analysis* (North-Holland, Amsterdam, 1970). However, we restrict ourselves to the case of large n for which the difference is negligible.
40. E. Arimondo and G. Orriols, *Lett. Nuovo Cimento* **17**, 333 (1976).
41. Paul Lett, National Institute of Standards and Technology, Gaithersburg, Md. 20899 (personal communication, 1992).